JMEPEG (2012) 21:2480–2486
DOI: 10.1007/s11665-012-0204-5

1059-9495/$19.00

Comparison of SCC Thresholds and Environmentally Assisted Cracking in 7050-T7451 Aluminum Plate

Eric M. Arnold, Joel J. Schubbe, Patrick J. Moran, and Robert A. Bayles

(Submitted January 9, 2012; in revised form February 20, 2012)

Aerospace alloys, often aluminums, are frequently exposed to corrosive environments resulting from naval service. These environments may produce significant changes in crack growth characteristics in these materials. An experiment was designed to characterize the effects of environment on crack growth thresholds and fracture characteristics for existing cracks in aluminum 7050-T7451 plate material. This data will be comparatively analyzed against aluminum 7075-T7631, an alloy with known susceptibility to corrosion, in order to determine a relative susceptibility of 7050-T7451, generally considered a superior aluminum alloy in terms of strength and corrosion resistance. The resulting data and subsequent analysis can in turn be used in more accurate determination of aircraft component service life in common corrosive environments experienced by aircraft in naval service.

Keywords aluminum alloys, aerospace vehicles, delamination, fatigue crack growth, fractography, fracture mechanics, mixed mode fracture

1. Introduction

Aircraft designers are constantly seeking materials which will provide the optimal performance to the aircraft which they design. Minimizing weight without sacrificing strength is one of the primary goals in selecting the best material for aviation applications. Resisting the effects of the environment is another important consideration. In the design of new military aircraft, titanium alloys are a primary structural choice due to their high strength to weight ratio and high resistance to corrosion. Historically, aluminums are frequently used in aerospace applications also due to their favorable strength to weight ratio and additionally, their relative low cost compared to that of alloys such as titaniums. In order to reduce weight and costs in manufacturing, designers are selecting new aluminum alloy products to include 7050 and 7075 series plate and forgings for use in aggressive stress and corrosive environments.

As an additional consideration, many aircraft components are being designed with, and constructed out of, thick and rolled plate products rather than forged castings in an attempt to reduce the high residual stresses generated in deep forgings and to reduce stress gradients due to forming processes. In several new aircraft designs, aluminum 7050-T7451 plate was selected as one of the primary structural alloy forms. This alloy, in thick plate form and considered a superior aluminum alloy, was selected prior to full characterization of fatigue cracking in all orientations, which could lead to potential life prediction problems in parts manufactured from this plate product. In previous studies, it was discovered that at load levels above a certain threshold, 7050-T7451 thick plate has the potential for crack splitting parallel to the load direction when loaded in the LS direction (Ref 1, 2). This poses a particular problem in components formed of plate products such as aircraft bulkheads, which have the potential to crack in directions which are neither expected nor easily evaluated, and which in turn hold the potential for reduced service life and unexpected failure. Inspection of such 'buried' parts is also problematic. As an added factor of concern, chemicals permeating the structure such as those contained in seawater, salt spray, and the various cleaners associated with naval-based aircraft should be evaluated both on pristine and flawed structure to determine susceptibility of these components to environmentally aggravated damage. Modes, mechanisms, and test methods are reviewed in Braun's works and supported through works of the National Association of Corrosion Engineers (Ref 3-5).

This study was designed to determine the effects of environment upon cracking within the 7050-T7451 alloy with pre-existing cracks. Specimens were exposed to 3.5% NaCl solution, which is the approximate concentration of seawater, as well as PENAIR M-5571, which is a common emulsifying cleaner used on naval aircraft. These environmental solutions are two of the most common experienced by aircraft in maritime environments and in the naval service.

Aluminum 7075-T7631 has historically proven to be an aluminum alloy susceptible to corrosion cracking, and as such, specimens were tested in the same manner and environments as those of 7050-T7451 (Ref 6). This allowed for direct comparison of the response of each alloy to the reagents used in this experiment, and thereby determine the relative susceptibility of 7050-T7451 to environmentally assisted cracking.

2. Test Setup and Data Collection

Twelve compact tension specimens were cut for this experiment from rolled plate aluminum products. The grain

Eric M. Arnold, Joel J. Schubbe, and **Patrick J. Moran**, Mechanical Engineering Department, US Naval Academy, 590 Holloway Road, Annapolis, MD 21402; and **Robert A. Bayles**, Naval Research Laboratory, 4555 Overlook Ave, SW, Washington, DC 20375. Contact e-mail: Schubbe@usna.edu.

structure for the 16.5 cm 7050-T7451 plate is shown in Fig. 1. All specimen dimensions were in accordance with ASTM standards as shown in Fig. 2 (Ref 7, 8). Of these 12 specimens, six were cut from aluminum 7050-T7451 in the longitudinal short-transverse or LS orientation allowing for crack splitting in the longitudinal direction, and the remaining six specimens were cut from 7075-T7631 in the longitudinal transverse or LT orientation (due to availability of material and documented comparison values). These specimens were fatigue pre-cracked using a MTS 810 electric servo-hydraulic 22 kip test stand.

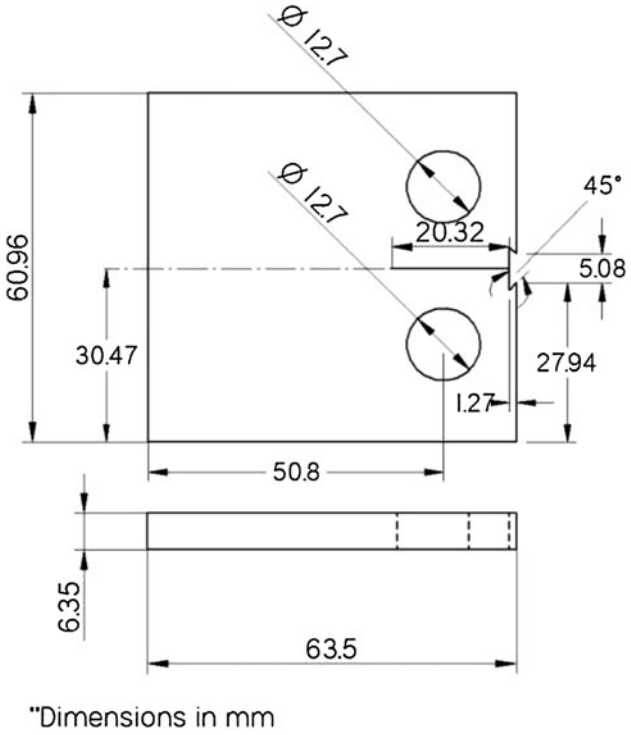

Fig. 1 ASTM Standard E399-08 compact tension specimen

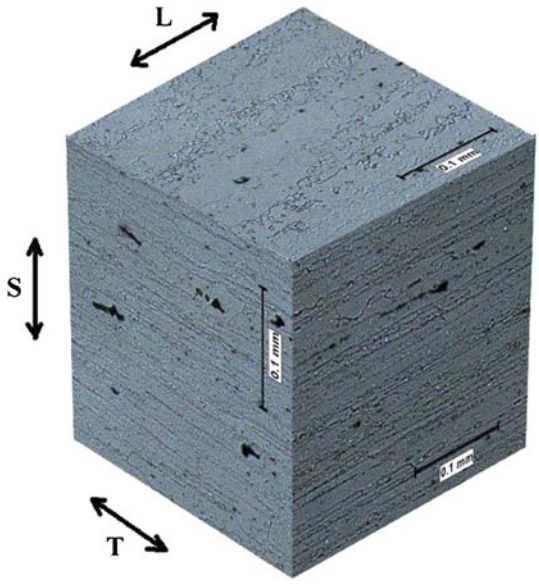

Fig. 2 Typical grain structure and orientation in 7050-T7451

An external MTS Flex SE Controller was used in conjunction with MTS PC interface software and Cyctest software in order to control the pre-cracking and maintain constant ΔK and a load ratio of $R = 0.1$ for each specimen. This pre-cracking was conducted well below previous documented threshold values for splitting progression in aluminums. A MTS clip gage was used to measure crack opening displacement (COD) throughout fatigue pre-cracking. The fatigue load was such that a tension-tension stress range of approximately 8.79 MPa$\sqrt{\text{m}}$ was applied at 10 Hz. Fatigue pre-cracking was stopped once a crack had been grown to an approximate length of 3.5 mm from the notch root as calculated using the crack closure compliance method. After fatigue pre-cracking, the specimens were statically pin loaded using the load jig shown in Fig. 3.

The crack closure compliance method was used to calculate the load required to reach an initial loading of 80% of K_{IC}. Due to the variability of the manual loading jig, the value below K_{IC} was used to prevent overloading of the specimen. It was found that this loading was sufficient to generate stable growth and achieve an experimental value for K comparison.

$$P = \frac{K_{\text{desired}}\sqrt{B^2}\sqrt{W}}{f\left(\frac{a}{W}\right)} \quad \text{(Eq 1)}$$

In Eq 1, P is the load, K_{desired} is 80% of the documented K_{IC} value, B is the thickness of the compact tension specimen, W is the specimen width, and $f\left(\frac{a}{W}\right)$ is a calibration function shown in Eq 2 where a is the distance from the specimen load line to the crack tip.

$$f\left(\frac{a}{W}\right) = \frac{\left(2+\frac{a}{W}\right)\left[0.886+4.64\left(\frac{a}{W}\right)-13.32\left(\frac{a}{W}\right)^2+14.72\left(\frac{a}{W}\right)^3-5.6\left(\frac{a}{W}\right)^4\right]}{\left(1-\frac{a}{W}\right)^{\frac{3}{2}}} \quad \text{(Eq 2)}$$

The COD that would result from this loading was also calculated using crack closure compliance equations of ASTM E399. With the MTS clip gage, the COD was used in conjunction with the load jig from Fig. 3 in order to apply the proper loading on the specimens (Ref 9).

$$V_m = \frac{P}{E_{\text{eff}}B_e}\cdot q\left(\frac{a}{W}\right) \quad \text{(Eq 3)}$$

In Eq 3 V_m is the COD of the specimen, E_{eff} is the effective modulus of elasticity, B_e is the effective specimen thickness, and q is a calibration function given by Eq 4.

$$q\left(\frac{a}{W}\right) = \frac{19.75}{\left(1-\frac{a}{W}\right)^2}\left[0.5+0.192\left(\frac{a}{W}\right)+1.385\left(\frac{a}{W}\right)^2 - 2.919\left(\frac{a}{W}\right)^3+1.842\left(\frac{a}{W}\right)^4\right] \quad \text{(Eq 4)}$$

$$E_{\text{eff}} = \frac{E}{1-\nu^2} \quad \text{(Eq 5)}$$

$$B_e = \frac{B-(B-B_N)^2}{B} \quad \text{(Eq 6)}$$

Equation 5 calculates the effective modulus in plane strain, where ν is Poisson's ratio for the material. In Eq 6 for the

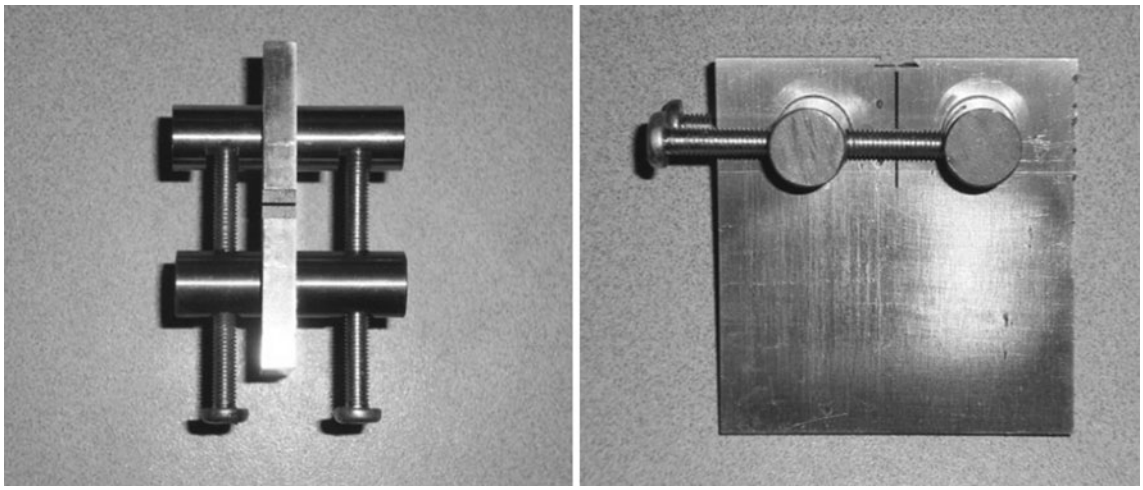

Fig. 3 Compact tension specimen with load jig installed to provide constant crack opening displacement

Table 1 Specimen test matrix with initial load applied to the specimen load line by pin loading

Specimen #	Alloy	Reagent	Initial loading (N)
AS-01	7050-T7451	3.5% NaCl	8010.35
AS-02	7050-T7451	3.5% NaCl	8105.66
AS-03	7050-T7451	3.5% NaCl	8034.70
BS-01	7075-T7631	3.5% NaCl	8453.79
BS-02	7075-T7631	3.5% NaCl	8552.47
BS-03	7075-T7631	3.5% NaCl	8587.73
AW-01	7050-T7451	PENAIR M-5571	8205.47
AW-02	7050-T7451	PENAIR M-5571	7994.18
AW-03	7050-T7451	PENAIR M-5571	7983.42
BW-01	7075-T7631	PENAIR M-5571	8629.14
BW-02	7075-T7631	PENAIR M-5571	8379.48
BW-03	7075-T7631	PENAIR M-5571	8593.62

Table 2 Fracture toughness of each test specimen at significant times over the course of the experiment

Specimen #	Documented K_{IC}	80% K_{IC}	$K_{threshold}$	K_{SCC}(a)
AS-01	35.05310733	28.0424859	27.998	27.949
AS-02	35.05310733	28.0424859	28.004	27.961
AS-03	35.05310733	28.0424859	28.022	27.993
BS-01	36.26183517	29.0094681	29.089	29.067
BS-02	36.26183517	29.0094681	28.922	28.853
BS-03	36.26183517	29.0094681	28.949	28.901
AW-01	35.05310733	28.0424859	28.011	27.979
AW-02	35.05310733	28.0424859	28.011	27.973
AW-03	35.05310733	28.0424859	28.035	27.986
BW-01	36.26183517	29.0094681	28.893	28.855
BW-02	36.26183517	29.0094681	29.087	29.064
BW-03	36.26183517	29.0094681	28.941	28.901

All K values are in units of MPa$\sqrt{m}$

(a) These values for K_{SCC} are those calculated from each of the specimens at a time approximately 1400 h after initial loading

effective specimen thickness, B_N is the thickness of the specimen at the base of a groove extending from the notch root. The specimens used in this study did not use such a groove resulting in $B_N = B$.

Once the above calculated load is applied, the crack begins to propagate in air as a result of the load. Periodic measurements of the crack length were taken using a Starett optical traveling telemicroscope with a digital readout to the ten-thousandth of an inch. These measured crack lengths were plotted versus time. The fixed COD maintained by the load jig and Eq 3 allowed calculation of the decreasing load (and thus K) on the specimen as the crack increased in length. After a period of approximately 330 h, crack growth slowed to a rate determined to be negligible. This arrest signified that the experimental threshold in air (or K_{IC}) for the specimen had effectively been reached (Ref 10).

After reaching K_{IC}, one of the two corrosive agents was periodically dripped on the notch root and crack on each face of the specimen. Two agents commonly found in naval aviation environments, 3.5% NaCl solution and PENAIR M-5571, an emulsifying aircraft cleaner at full strength, were used in this experiment. The specimens were tested in triplicates with three specimens of each alloy being exposed to each of the drip solutions. The test specimen matrix for this experiment is shown in Table 1.

When applying the environment to the specimen, one drop of solution was applied to the notch root and crack area on the front face of each specimen using a needle-less syringe. The solution was drawn to the crack tip by capillary action before excess solution was wiped from the face of the specimen in order to reduce the potential for pitting or other corrosion on the surface of the specimen which would obscure the crack and make optical measurement difficult. After allowing the droplet of solution to remain on the specimen for a period of 1-2 min, the surface was wiped clean and a drop was applied to the other face. The same procedure was followed on the other side of each specimen, and the crack length was measured on both sides. These values were averaged together assuming that the crack tip is linear through the thickness of the specimen and growing in a self-similar manner. Measurements showed no significant evidence to the contrary. Specimens were exposed to their respective environments on a daily basis for a period of approximately 1400 h.

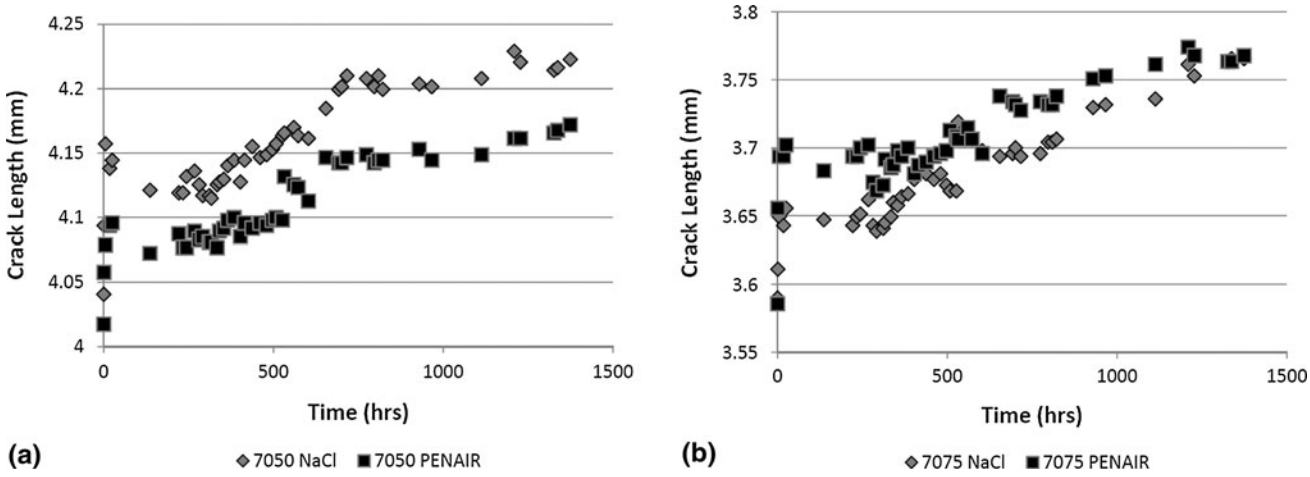

Fig. 4 Crack length over time including initial loading and pop-in crack growth, continued crack growth to arrest at experimental threshold K_{IC}, and crack growth as a result of environmental exposure over the period between 330 and 1400 hours for (a) 7050-T7451 and (b) 7075-T7631

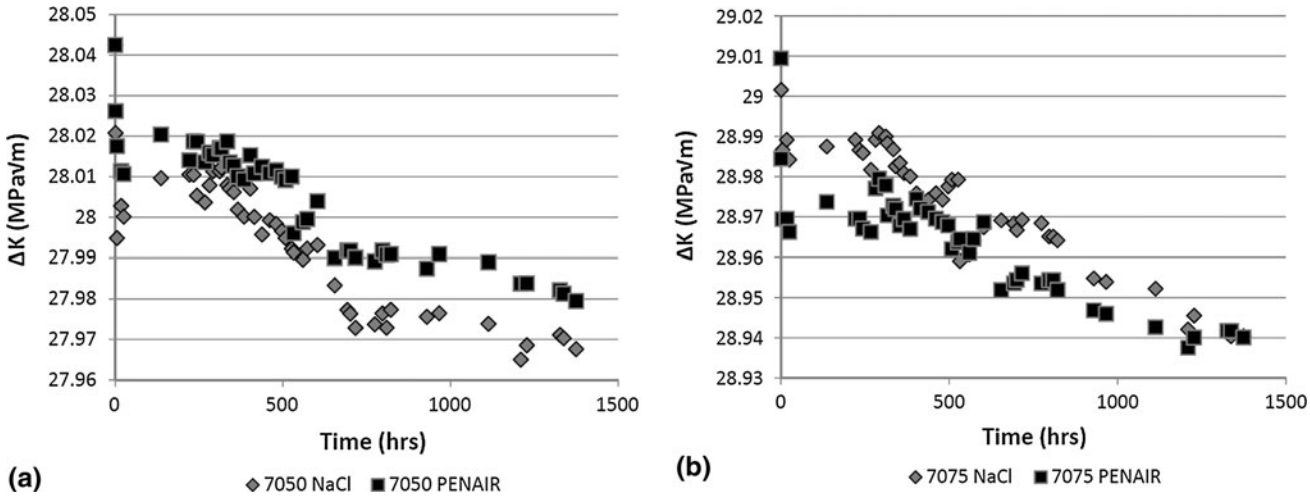

Fig. 5 ΔK values plotted over time showing the experimental threshold prior to 330 h in (a) 7050-T7451 and (b) 7075-T7631

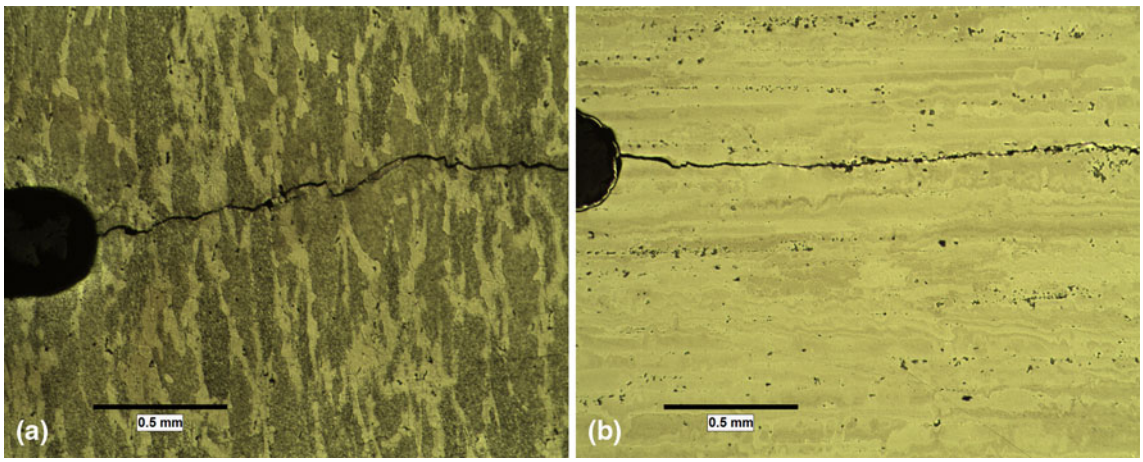

Fig. 6 Representative photographs of cracking in each alloy. (a) 50× magnification of typical crack in 7050-T7451. (b) 50× magnification of a typical crack in 7075-T7631

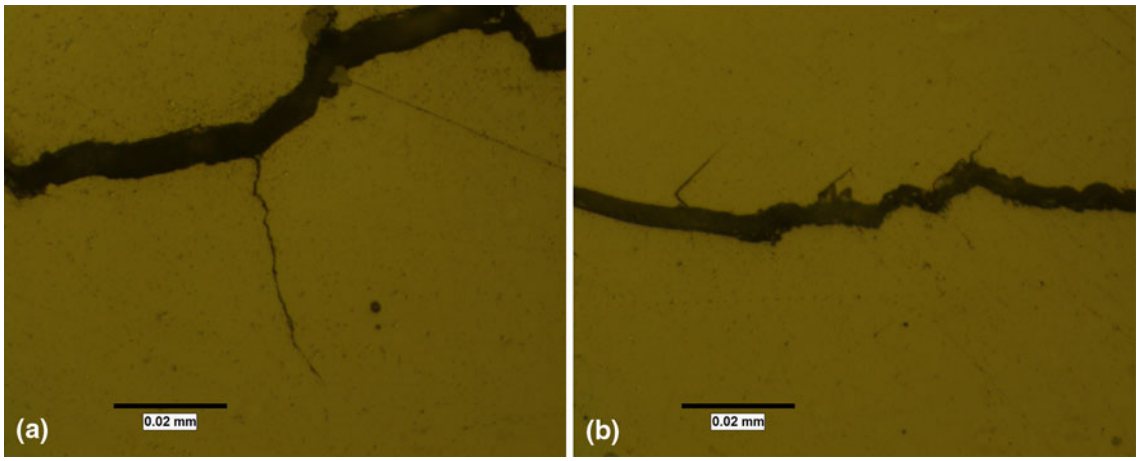

Fig. 7 (a) 1000× magnification of splitting and secondary cracking in 7050-7451. (b) 1000× magnification of splitting and secondary cracking in 7075-T7631

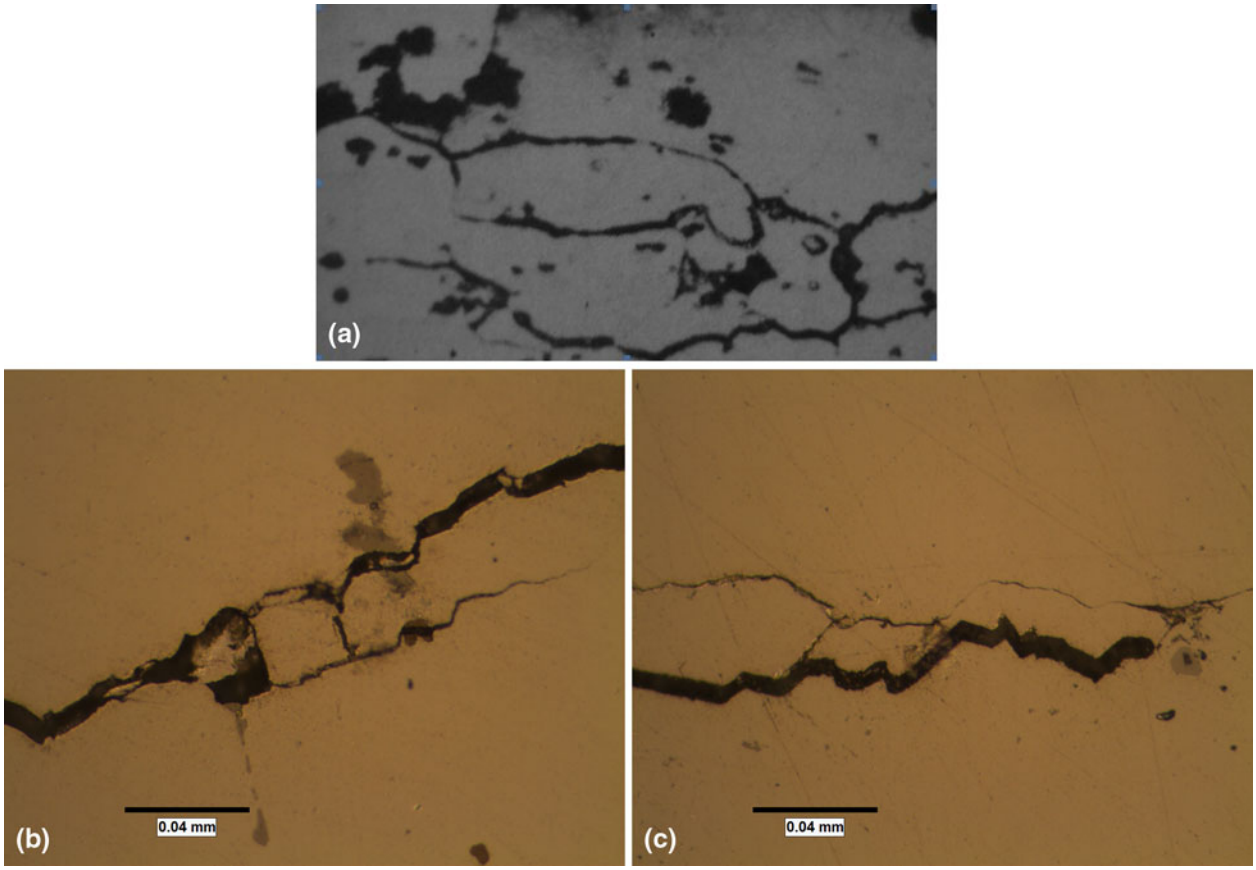

Fig. 8 Stress corrosion cracking. (a) Documented example in aluminum 2014-T6 at 250× magnification (Ref 8). (b) 500× magnification micrograph of 7050-T7451. (c) 500× magnification micrograph of 7075-T7631

3. Results and Discussion

3.1 Experimental Crack Growth

Each of the 12 specimens experienced detectable crack growth after loading to 80% of the documented value for K_{IC}. Crack growth, at constant COD, resulted in decreased specimen load at the load line, as well as a drop in the calculated ΔK. After a period of approximately 330 h, this crack growth arrested at an experimental threshold ΔK. As the reagents were applied to the specimens, detectable crack propagation resumed as a result of exposure to these environments causing subsequent drops in load

and ΔK. The ΔK values for each specimen at each of the significant events within the experiment are contained within Table 2.

The total primary direction crack length of each specimen was optically measured over a period of approximately 1400 h. In that time detectable cracking as a result of exposure to environment occurred in both the 7050-T7451 and 7075-T7631 specimens in both 3.5% NaCl and PENAIR M-5571. The average crack length in each triplicate is plotted in Fig. 4 showing the crack propagation over the course of the experiment. The K values for each specimen resulting from the observed crack length are plotted in Fig. 5.

The K values listed in Table 2 and plotted in Fig. 5 were calculated using the crack closure compliance method, Eq 1, which, in the case of this experiment provides an approximation of the drop in K as calculated from the measurement of the primary crack growth. However, this method cannot account for any branching or splitting in the crack. Such anomalies would increase the effective crack length, decreasing the resulting calculated applied load and value of K. A minimal decrease in K was observed, typically on the order of 0.1-0.2%.

3.2 Metallographic Examination

Post-test metallographic imaging showed that the splitting and branching was occurring and therefore the resulting threshold values may be significantly lower than plotted and

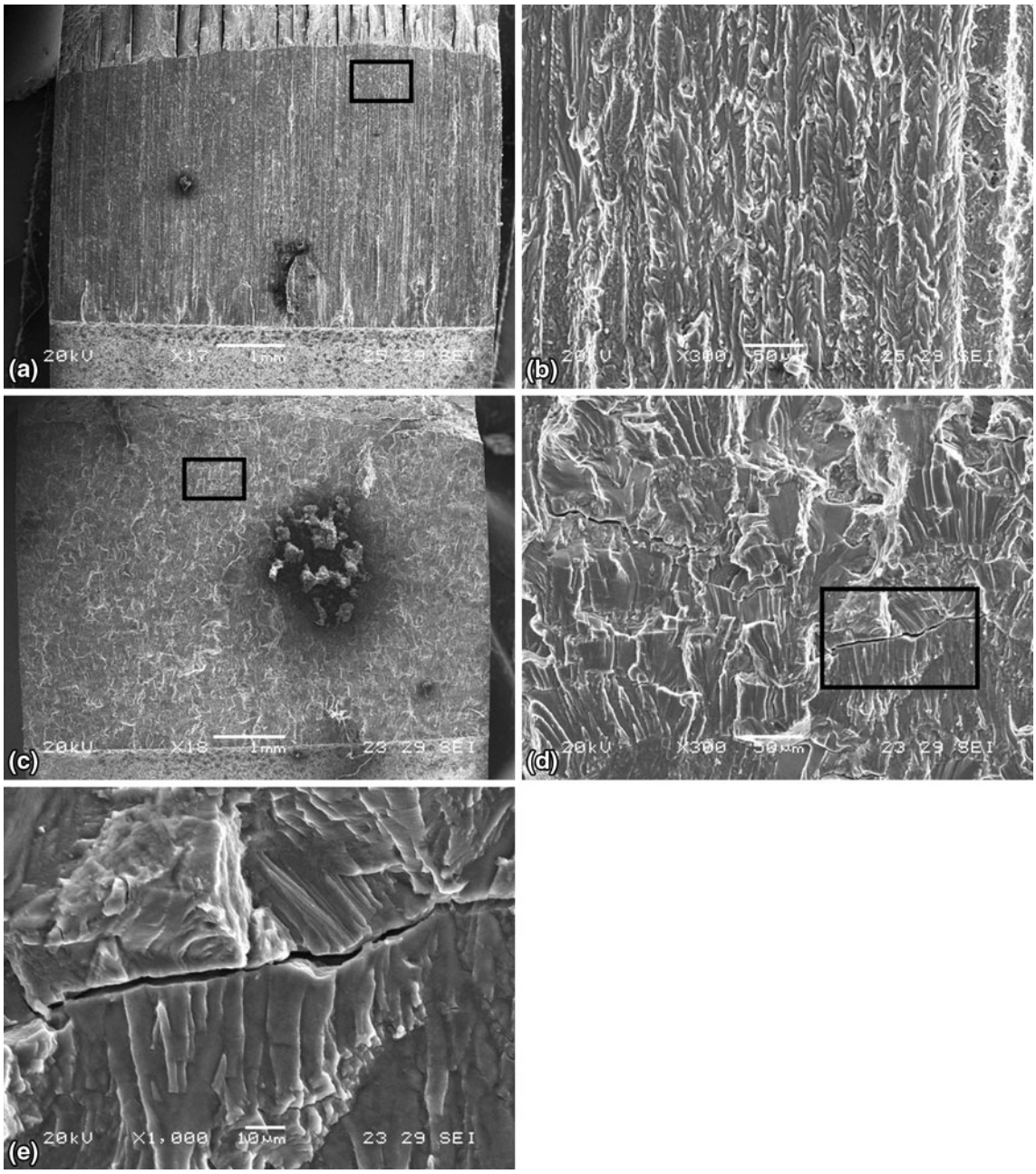

Fig. 9 (a) 17× magnification of 7075-T7631 specimen fracture surface. (b) 300× magnification of stress corrosion cracking region of 7075-T7631 specimen. (c) 18× magnification of 7050-T7451 specimen fracture surface. (d) 300× magnification of stress corrosion cracking region and secondary cracking of 7050-T7451 specimen. (e) 1,000× magnification of secondary cracking in 7050-T7451

the effective decrease and percentage change in K may be much greater. Representative photographs of typical cracking observed in each of the test alloys are shown in Fig. 6. Test groups of the same alloy exhibited very similar behavior in both adverse environments, so Fig. 6 compares the two alloys rather than attempting a comparison between the environments. Both test alloys experienced splitting and secondary cracking under exposure to both reagents, but this splitting was significantly greater in 7050-T7451 than in 7075-T7631. Secondary cracks in 7050 were typically four to five times the length of their counterparts in 7075. Representative photographs of this behavior are also included in Fig. 6 and 7.

Stress corrosion cracking is often characterized by fine, deeply penetrating cracks which exhibit little to no corrosion on the surface of the metal. Cracking resulting from stress corrosion ordinarily exhibit branching and splitting perpendicular to the applied load (Ref 11, 12). Figure 8 shows an accepted example of stress corrosion cracking in aluminum in comparison with the cracking behavior seen in test specimen of 7050-T7451 and 7075-T7631 from this study.

The fracture surface of one specimen from each test triplicate was examined using scanning electron microscopy. This examination provided further evidence that 7050-T7451 exhibits significant crack branching and stress corrosion cracking. Representative SEM fractographs are shown in Fig. 9a-e.

4. Conclusions

A viable method for examining the effects of adverse environments on existing cracks was employed to examine the susceptibility of 7050-T7451 thick plate to environmentally assisted or enhanced cracking. It was shown that detectable growth was achieved and was compared to a known susceptible alloy 7075-T7631. The specimens of 7075-T7631 experienced detectable crack growth as a result of exposure to both 3.5% NaCl and PENAIR M-5571 which exhibited the characteristics of stress corrosion cracking. This confirms the susceptibility of this alloy to environmentally assisted cracking and confirms its usefulness as a benchmark against which to compare the behavior of 7050-T7451. The latter alloy also experienced detectable crack growth in response to the application of reagents to the crack tip. As a result, 7050-T7451 also has a small but present susceptibility to corrosion cracking in this L-S orientation. As such, its use as a structural alloy should be carefully monitored, and further studies should be conducted to further characterize the fracture behavior of this alloy.

Additionally, the 7050-T7451 exhibited the tendency for cracks to split perpendicular to the primary crack growth direction or branch in an unpredictable manner. This behavior was first exhibited during previous studies characterizing fatigue fracture of the material. The presence of this behavior under environmental cracking conditions calls for considerable evaluation of this thick material plate product as a structural aerospace alloy. Such behavior poses a major threat in that cracks of significant size may be propagating through currently in-service aircraft components in directions or locations which may be much more difficult to find and evaluate.

Further examination of this subject will likely include a granular analysis of each of the test alloys, particularly investigating fracture method and element concentrations along the grain boundaries. Further study is planned to include additional orientations of the alloys in question. A similar study of 5083 series aluminum plate is also underway using these test methods.

Acknowledgments

The authors thank the Center for Corrosion Science and Engineering, United States Naval Research Laboratory, Washington, DC.

References

1. J. Schubbe, Evaluation of fatigue life and crack growth rates in 7050-T7451 aluminum plate for T-L and L-S oriented failure under truncated spectra loading, *Eng. Fail. Anal.*, 2009, **16**, p 340–349
2. J. Schubbe, Fatigue Crack Propagation in 7050-T7451 Plate Alloy, *Eng. Fract. Mech.*, 2009, **76**, p 1037–1048. doi:10.1016/j.engfracmech.2009.01.006
3. R. Braun, Environmentally Assisted Cracking of Aluminum Alloys, *Mat.-wiss. u. Werkstofftech.*, 2007, **38**(9), doi:10.1002/mawe.200700204
4. N. Holroyd, Environment-Induced Cracking of High-Strength Aluminum Alloys, *Proceedings of the First International Conference on Environment-Induced Cracking of Metals*, R.P. Gangloff, M.B. Ives, Ed., 1988, NACE-10, National Association of Corrosion Engineers, Houston TX, 1990, p 311–345
5. D. Sprowls, *Fundamental Aspects of Stress Corrosion Cracking*, R.W. Staehle, Ed., National Association of Corrosion Engineers, Houston, 1969, p 466
6. E. Hollingsworth and B. Hunsicker, *Metals Handbook*, Vol 13, 9th ed., ASM International, Metals Park, OH, 1987
7. ASTM Standard E399-08, "Standard Test Method for Linear-Elastic Plane-Strain Fracture Toughness KIC of Metallic Materials", ASTM International, West Conshohocken, PA, 2008, www.astm.org
8. ASTM Standard E647-08, "Standard test method for measurement of fatigue crack growth rates," ASTM International, West Conshohocken, PA, 2008, www.astm.org
9. S. Antolovich and B. Antolovich, *ASM Handbook: Fatigue and Fracture*, Vol 19, ASM International, Materials Park, OH, 1996, p 371–392
10. R. Gangloff, R. Piascik, D. Dicus, and J. Newman, Fatigue Crack Propagation in Aerospace Aluminum Alloys, *J. Aircraft*, 1994, **31**, p 720–729
11. B.E. Wilde, *ASM Handbook: Failure Analysis and Prevention*, Vol 11, ASM International, Materials Park, OH, 1986, p 203–224
12. G. Koch, *ASM Handbook: Fatigue and Fracture*, Vol 19, ASM International, Materials Park, OH, 1996, p 483–506